

NUCLEAR REACTIONS IN MONTE CARLO CODES

Alfredo Ferrari^{#,†,*} and Paola R. Sala^{&,†}

[#] European Laboratory for Particle Physics (CERN), CH-1211 Geneva 23, Switzerland

[&] ETH Zürich, CH-8093 Zürich, Switzerland

[†] on leave from INFN Milan, Via Celoria 16 20133 Milan, Italy

Received:

Abstract – The physics foundations of hadronic interactions as implemented in most MonteCarlo codes are presented together with a few practical examples. The description of the relevant physics is presented schematically split into the major steps in order to stress the different approaches required for the full understanding of nuclear reactions at intermediate and high energies. Due to the complexity of the problem, only a few semi-qualitative arguments are developed in this paper. The description will be forcibly schematic and somewhat incomplete, but it will be hopefully useful for a first introduction into this topic. Examples are shown mostly for the high energy regime, where all mechanisms mentioned in the paper are at work and perhaps most of the readers are less used at. Examples for lower energies can be found in the references.

* Contact author E-mail: Alfredo.Ferrari@cern.ch

INTRODUCTION

A very first question about MonteCarlo modelling of nuclear interactions could be, why MonteCarlo and not different approaches? Actually the MonteCarlo approach to nuclear reactions has several advantages when used in full transport radiation codes.

The typical advantages of a MonteCarlo approach are listed in the following: a few are common to other approaches, however only the MonteCarlo method can provide all of them when properly implemented

- Theory driven and data benchmarked
- Naturally extended to materials/energies where no data are available
- Natural accounting for non-measured secondaries
- Event-by-event description, with full correlations and exact energy conservation, provided analogue, self-consistent models are used both for interaction modelling and particle transport
- Description of complex geometries, including time-varying problems
- Transport in electric and magnetic fields
- Fully three-dimensional calculations
- Variance reduction by biasing techniques

There are of course limitations, mostly:

- Computer time: convergence $\propto 1/\sqrt{N}$
- Model complexity sometimes limited by CPU requirements
- Not all theoretical models can be translated into MC algorithms

MAIN STEPS OF H-A INTERACTIONS

The approach to hadronic interaction modelling presented here is the one adopted by most state-of-the-art codes. In this “microscopic” approach, each step has sound physical basis. Performances are optimized comparing with particle production data at single interaction level. No tuning whatsoever on “integral” data, like calorimeter resolutions, thick target yields etc, is performed. Therefore, final predictions are obtained with minimal free parameters, fixed for all energies and target/projectile combinations. Results in complex cases as well as scaling laws and properties come out naturally from the underlying physical models and the basic conservation laws are fulfilled “a priori”. All the examples/results presented in the following have been obtained with FLUKA ^(1,2,3) and should be typical of codes adopting similar approaches.

High-energy hadron-nucleus (h-A) interactions can be schematically described as a sequence of the following steps:

- Glauber-Gribov cascade and high energy collisions
- (Generalized)-IntraNuclear cascade
- Preequilibrium emission
- Evaporation/Fragmentation/Fission and final deexcitations

Individual aspects of the interaction simulation can be of particular relevance for some applications rather than for others: for example those critical for calorimetry applications are discussed in ⁽⁴⁾. However the overall coherence of a successful model is based on its ability to describe very different problems within the same, self-consistent, physics approach.

Before briefly discussing each individual step, a few words about the modelling of hadron-nucleon collisions are required in order to understand more complex hadron-nucleus or nucleus-nucleus collisions.

1. HADRON-NUCLEON INTERACTION MODELS

A comprehensive understanding of hadron-nucleon interactions over a large energy range is of course a basic ingredient for a sound description of hadron-nucleus ones. Elastic, charge exchange and strangeness exchange reactions, are described as far as possible by phase-shift analysis and/or fits of experimental differential data. Standard eikonal approximations are often used at high energies.

At the low energy end (below 100 MeV) the p-p and p-n cross sections are rapidly increasing with decreasing energy. There is a factor three at the lowest energies between the n-p and the p-p cross sections, as expected on the basis of symmetry and isospin considerations, while at high energies they tend to be equal.

The total cross section for the two isospin components present in the nucleon-nucleon amplitude is given by:

$$\begin{aligned}\sigma_T^1 &= \sigma_{pp} \\ \sigma_T^0 &= 2\sigma_T^{np} - \sigma_T^{pp}\end{aligned}$$

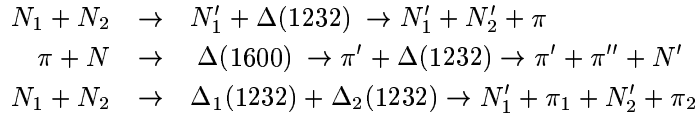
The same decomposition can be shown to apply for the elastic and the reaction cross sections too.

The cross section for pion-nucleon scattering is dominated by the existence of several direct resonances, the most prominent one being the $\Delta(1232)$. Given the pion isotopic spin ($T = 1$), the three π charge states correspond to the three values of T_z . Thus, in the pion-nucleon system two values of T are allowed: $T = \frac{1}{2}$ and $T = \frac{3}{2}$, and two independent scattering amplitudes, $A_{\frac{1}{2}}$ and $A_{\frac{3}{2}}$, enter in the cross sections. Using Clebsch-Gordan coefficients all differential cross sections can be derived from the three measured ones: $\sigma(\pi^+p \rightarrow \pi^+p)$, $\sigma(\pi^-p \rightarrow \pi^-p)$, $\sigma(\pi^-p \rightarrow \pi^0n)$.

As soon as particle production (inelastic hadron-nucleon interactions) are concerned, the description becomes immediately more complex. Two families of models are adopted, depending on the projectile energy, those based on individual resonance production and decays, which cover the energy range up to 3-5 GeV, and those based on quark/parton string models, which can provide reliable results up to several tens of TeV.

(1) H-N INTERACTIONS AT INTERMEDIATE ENERGIES

The lowest threshold inelastic channel, single pion production, opens already around 290 MeV in nucleon-nucleon interactions, and becomes important above 700 MeV. In pion-nucleon interactions the production threshold is as low as 170 MeV. Both reactions are normally described in the framework of the isobar model: all reactions proceed through an intermediate state containing at least one resonance. There are two main classes of reactions, those which form a resonant intermediate state (possible in π -nucleon reactions) and those which contain two particles in the intermediate state. The former exhibit bumps in the cross sections corresponding to the energy of the formed resonance. Examples are reported below:



Partial cross sections can be obtained from one-boson exchange theories and/or folding of Breit-Wigner with matrix elements fixed by N-N scattering or experimental data. Resonance energies, widths, cross sections, branching ratios are extracted from data and conservation laws, whenever possible, making explicit use of spin and isospin relations. They can be also inferred from inclusive cross sections when needed.

For a discussion of resonance production, see for example ^(5,6,7).

(2) INELASTIC HN INTERACTIONS AT HIGH ENERGIES: (DPM, QGSM, ...)

As soon as the projectile energy exceeds a few GeV's, the description in terms of resonance production and decay becomes more and more difficult. The number of resonances which should be considered grows exponentially and their properties are often poorly known. Furthermore, the assumption of one or two resonance creation is unable to reproduce the experimental finding that most of the particle production at high energies occurs neither in the projectile or target fragmentation region, but rather in the central region, for small values of Feynmann X variable. Different models, based directly on quark degrees of freedom must be introduced.

The features of "soft" interactions (low- p_T interactions) cannot be derived from the QCD Lagrangian, because the large value taken by the running coupling constant prevents the use of perturbation theory. Models based on interacting strings emerged as a powerful tool in understanding QCD at the soft hadronic scale, that is in the non-perturbative regime. An interacting string theory naturally leads to a topological expansion. The Dual Parton Model ⁽⁸⁾ is one of these models (another, very similar, example is the Quark-Gluon-String-Model ^(9,10)) and it is built introducing partonic ideas into a topological expansion which explicitly incorporates the constraints of duality and unitarity, typical of Regge's theory. In DPM hadrons are considered as open strings with quarks, antiquarks

or diquarks sitting at the ends; mesons (colorless combination of a quark and an antiquark $q\bar{q}$): are strings with their valence quark and antiquark at the ends. At sufficiently high energies the leading term in the interactions corresponds to a Pomeron (IP) exchange (a closed string exchange), which has a cylinder topology. When an unitarity cut is applied to the cylindrical Pomeron two hadronic chains are left as the sources of particle production. As a consequence of color exchange in the interaction, each colliding hadron splits into two colored system, one carrying color charge c and the other \bar{c} . The system with color charge c (\bar{c}) of one hadron combines with the system of complementary color of the other hadron, to form two color neutral chains. These chains appear as two back-to-back jets in their own centre-of-mass systems.

The exact way of building up these chains depends on the nature of the projectile-target combination (baryon-baryon, meson-baryon, antibaryon-baryon, meson-meson): examples are shown in figs. 1, and 2: further details can be found in the original DPM references ⁽⁸⁾ or in ⁽³⁾.

The chains produced in an interaction are then hadronized. DPM gives no prescriptions on this stage of the reaction. All the available chain hadronization models, however, rely on the same basic assumptions, the most important one being *chain universality*, that is chain hadronization does not depend on the particular process which originated the chain, and that until the chain energy is much larger of the mass of the hadrons to be produced, the fragmentation functions (which describe the momentum fraction carried by each hadron) are the same. As a consequence, fragmentation functions can in principle be derived from hard processes and e^+e^- data and the same functions and (few) parameters should be valid for all reactions and energies; actually mass and threshold effects are non-negligible at the typical chain energies involved in hadron-nucleus reactions. Transverse momentum is usually added according to uncertainty considerations. The examples in figs. 3,4 show the ability of the FLUKA, DPM based, model to reproduce the features of particle production; further examples can be found in ^(1,3).

2. (GENERALIZED) INTRANUCLEAR CASCADE BASIC ASSUMPTIONS

At energies high enough to consider coherent effects as corrections, a hadron-nucleus (hA) reaction can be described as a cascade of two-body interactions, concerning the projectile and the reaction products. This is the mechanism called IntraNuclearCascade (INC). INC models were developed already at the infancy of the computer era with great success in describing the basic features of nuclear interactions in the 0.2-2 GeV range. Modern INC models had to incorporate many more ideas and effects in order to describe in reasonable way reactions at higher and lower energies. Despite particle trajectories are described classically, many quantistic effects have to be incorporated in these (Generalized)INC models, like Pauli blocking, formation time, coherence length, nucleon antisymmetrization, hard core nucleon correlations. A thorough description of the (G)INC model used in FLUKA can be found in ^(1,3).

3. h-A AT HIGH ENERGIES: THE GLAUBER-GRIBOV CASCADE

The Glauber^(12,13) formalism provides a powerful and elegant method to derive elastic, quasi-elastic and absorption hA cross sections from the free hadron-Nucleon cross section and the nuclear ground state *only*. Inelastic interactions are equivalent to multiple interactions of the projectile with ν target nucleons. The number of such "primary" interactions follows a binomial distribution (at a given impact parameter, b):

$$P_{r\nu}(b) \equiv \binom{A}{\nu} P_r^\nu(b) [1 - P_r(b)]^{A-\nu}$$

where $P_r(b) \equiv \sigma_{hN} T_r(b)$, and $T_r(b)$ is the profile function (folding of nuclear density and scattering profiles along the path). On average :

$$\langle \nu \rangle = \frac{Z\sigma_{hp} r + N\sigma_{hn} r}{\sigma_{hA} abs}$$

$$\sigma_{hA} abs(s) = \int d^2\vec{b} \left[1 - (1 - \sigma_{hN} r(s) T_r(b))^A \right]$$

The Glauber-Gribov^(14,15,16) model represents the diagram interpretation of the Glauber cascade. The ν interactions of the projectile originate 2ν chains, out of which 2 chains (valence-valence chains) struck between the projectile and target valence (di)quarks, $2(\nu - 1)$ chains (sea-valence chains) between projectile sea $q - \bar{q}$ and target valence (di)quarks.

A pictorial example of the chain building process is depicted in fig. 5 for p-A: similar diagrams apply to π -A and \bar{p} -A respectively.

The distribution of the projectile energy among many chains naturally softens the energy distributions of reaction products and boosts the multiplicity with respect to hadron-hadron interactions (see fig. 6). The building up of the multiplicity distribution from the multiple collisions can be appreciated from fig. 7, where the multiplicity distribution for Al and Au targets at 250 GeV/c are presented together. In this way, the model accounts for the major A-dependent features without any degree of freedom, except in the treatment of mass effects at low energies.

The Fermi motion of the target nucleons must be included to obtain the correct kinematics, in particular the smearing of p_T distributions. All nuclear effects on the secondaries are accounted for by the subsequent (G)INC.

4. FORMATION ZONE

The Formation Zone concept is essential to understand the observed reduction of the re-interaction probability with respect of the naive free cross section assumption. It can be understood as a “materialization” time. A qualitative estimate can be given as follows: in the frame where $p_{\parallel} = 0$, the time necessary for materialization \bar{t} is

$$\bar{t} = \Delta t \approx \frac{\hbar}{E_T} = \frac{\hbar}{\sqrt{p_T^2 + M^2}}$$

Going to lab system

$$t_{lab} = \frac{E_{lab}}{E_T} \bar{t} = \frac{\hbar E_{lab}}{p_T^2 + M^2}$$

The condition for possible re-interaction inside a nucleus is:

$$v \cdot t_{lab} \leq R_A \approx r_0 A^{\frac{1}{3}}$$

At high energies, the “fast” (from the emulsion language) particles produced in the Glauber cascade have a high probability to materialize already outside the nucleus without triggering a secondary cascade. Only a small fraction of the projectile energy is thus left available for the INC and the evaporation (see fig.8 and par. 7.).

5. PREEQUILIBRIUM

At energies lower than the π production threshold a variety of preequilibrium models have been developed⁽¹⁹⁾ following two leading approaches: the quantum-mechanical multistep model and the exciton model. The former has very good theoretical background but is quite complex, while the latter relies on statistical assumptions, and it is simple and fast. Exciton-based models are often used in MonteCarlo codes to join the INC stage of the reaction to the equilibrium one (see ⁽³⁾ for the FLUKA implementation).

6. EVAPORATION, FISSION AND NUCLEAR BREAK-UP

At the end of the reaction chain, the nucleus is a thermally equilibrated system, characterized by its excitation energy. This system can “evaporate” nucleons, or fragments, or γ rays, or even fission, to dissipate the residual excitation. The evaporation and fission probability for a particle of type j , mass m_j , spin $S_j \cdot \hbar$ and kinetic energy E are given by⁽²⁰⁾

$$P_j = \frac{(2S_j + 1)m_j}{\pi^2 \hbar^3} \int_{V_j}^{U_i - Q_j - \Delta_f} \sigma_{inv} \frac{\rho_f(U_f)}{\rho_i(U_i)} E dE$$

$$P_F = \frac{1}{2\pi \hbar} \frac{1}{\rho_i(U_i)} \int_0^{(U - B_F)} \rho_F(U - B_F - E) dE$$

Where ρ 's are the nuclear level densities, U_i and U_f are the excitation energy of the initial and final nuclei, B_F is the fission barrier, Q_j the reaction Q for emitting a particle of type j , and σ_{inv} is the cross section for the inverse process, which takes into account a possible Coulomb barrier. Under standard approximations, the evaporation spectrum has a maxwellian shape:

$$P_j(E) dE \approx K E e^{-\frac{E}{T}} dE$$

where T ($T \approx \sqrt{(U - \Delta)/a}$) is the nuclear temperature, usually in the MeV range (a : level density parameter $\approx A/8 \text{ MeV}^{-1}$, Δ : pairing energy).

Neutron emission is favored over charged particle emission, due to the Coulomb barrier, especially for medium-heavy nuclei. Moreover, the excitation energy is higher in heavier nuclei due to the larger cascading chances and larger number of primary collision in the Glauber cascade at high energies, and a is smaller, thus the average neutron

energy is smaller. Therefore, the neutron multiplicity is higher for heavy nuclei than for light ones. For light residual nuclei, where the excitation energy may overwhelm the total binding energy, a statistical fragmentation (Fermi Break-up) model is more appropriate (see ^(1, 3, 21) for the FLUKA implementation).

The evaporation/fission/break-up processes represent the last stage of a nuclear interaction and are responsible for the exact nature of the residuals left after the interactions. However, for a coherent self-consistent model, the mass spectrum of residuals is highly constrained by the excitation energy distribution found in the slow stages, which in turn is directly related to the amount of primary collisions and following cascading which took place in the fast stages.

7. H-A AT HIGH ENERGIES: THE INVARIANCE OF THE TARGET FRAGMENTATION REGION

The description of nuclear interactions as a sequence of well defined physics processes, each one governed by its own laws, is very useful in understanding the complex dynamics of these collisions, and it leads also to a natural MonteCarlo implementation, where each stage is starting from the final state of the previous one. The power of this approach will be demonstrated in the following where the most basic properties of hadron-nuclear collisions in the multi-GeV range are explained by means of the concepts introduced in the previous sections.

The Glauber cascade and the formation zone act together in reaching a regime where the “slow” part of the interaction is almost independent of the particle energy. This can be easily verified looking at charged particle average multiplicities and multiplicity distributions as a function of energy (fig.8). “Fast” (or “shower”) tracks (charged particles with $\beta = \frac{v}{c} > 0.7$), coming from the projectile primary interactions, show the typical \approx logarithmic increase observed for hN interactions. As shown already in fig. 6 and fig. 7, the average multiplicity and its variance are directly related to the distribution of primary collisions as predicted by the Glauber approach. Due to the very slow variation of hadron-nucleon cross section from a few GeV up to a few TeV's, the Glauber cascade is almost energy independent and the rise in the multiplicity of “fast” particles is related only to the increased multiplicity of the elementary h-N interactions.

Due to the onset of formation zone effects, most of the hadrons produced in the primary collisions escape the nucleus without further reinteractions. Further cascading only involves the slow fragments produced in the target fragmentation region of each primary interaction, and therefore it tends to quickly saturate with energy as the Glauber cascade reaches its asymptotic regime. This trend is well reflected in the average multiplicity (and multiplicity distribution) of “gray” tracks (charged particles with $0.3 < \beta < 0.7$), which are mostly protons produced in secondary collisions during the intranuclear cascade and preequilibrium phases.

At the end of the cascading process, the residual excitation energy is directly related to the number of primary and secondary collision which took place. Each collision is indeed leaving a “hole” in the Fermi sea which carries an excitation energy related to its depth in the Fermi sea. According to the considerations outlined in the previous paragraphs, evaporation products, as well as residual excitation functions should reach an almost constant condition as soon as the Glauber mechanism and the formation zone are fully developed. This can indeed be verified looking at the production of “black” tracks (charged particles with $\beta < 0.3$), which are mostly evaporation products. The data reported in fig. 8 do indeed demonstrate how they saturate as well, and how this property is nicely reproduced by models based on the assumptions outlined in this paper.

The ultimate nature of the residual left after an interaction depends also on complicate details of nuclear structure which are often difficult to include in a MonteCarlo approach. In particular spin and parity dependent calculations are unmanageable due to their complexity, and anyway they would be pretty useless due to the impossibility of accounting for these quantum numbers in the fast stages of the reactions. Nevertheless the general features of isotope production are reasonably reproduced: in fig. 9 the computed and measured mass distributions of residuals after 300 GeV proton interactions on Silver, and 800 GeV protons on Gold are shown. The agreement is fairly good in the spallation region close to the target mass, and still reasonable down to very light masses where the observed discrepancy is due more to the lack of a fragmentation model in the calculation than to deficiencies in the physics of the fast stages.

Recent examples of successful applications to complex problems of models like those described in this paper can be found in ^(24, 25, 26).

NUCLEUS-NUCLEUS COLLISIONS

The topic of ion-ion nuclear interactions is very wide and cannot be treated in an exhaustive way in an introductory paper like the present one.

Only a few hints will be given in the following for a proper generalization of intranuclear cascade approach to nucleus-nucleus collisions.

1. THE APPROACH TO NUCLEUS-NUCLEUS CASCADING

In the intermediate energy range (≈ 100 MeV/n to few GeV/n), as well for the cascade part of high energy reactions, three main classes of microscopic models are suitable for MonteCarlo applications. These are all microscopic kinetic models including the propagation and mutual interactions of pion and nucleon resonances. Similar two body collision terms, mostly based on free scattering, are used for individual hadron-hadron collisions in strict analogy with the hadron-nucleus case. The three approaches differ mostly for the treatment of the nuclear field and the corresponding propagation of particles in the nuclear medium.

- (Generalized)IntraNuclear Cascade models
 - Nucleon mean field
 - semi-classical trajectories
- Quantum Molecular Dynamics models ^(30, 31)
 - Gaussian packet wave functions for nucleons
 - Nucleon mean field as the sum of two-body potentials
- BUU (Boltzmann-Uehling-Uhlenbeck) eq. based models ^(32, 33, 34, 35)
 - Time evolution equation of the nucleon (pions...) one-body phase-space distribution
 - Test particle method (semiclassical trajectories in a self-consistent mean field)

(G)INC and QMD models have been successfully implemented into MonteCarlo generators and sometimes extended up to very high energies (see for example ^(36, 37, 38, 39, 40, 41, 42, 31)) and to the treatment of all hadrons by means of the Glauber approach extended to AA collisions and of string models (like DPM).

2. THE GLAUBER FORMULATION FOR A-A COLLISIONS

The extension of the Glauber approach to nucleus-nucleus collisions is a classical approach and the details can be easily found in the literature (ie. ^(27, 28, 29)).

When extended to nucleus-nucleus collisions, the Glauber quantum mechanical approach leads to (B and A nucleons for the projectile/target respectively):

$$\begin{aligned}
 \sigma_{BA\ abs}(s) &\equiv \sigma_{BA\ T}(s) - \sigma_{BA\ el}(s) - \sigma_{BA\ qe}(s) = \\
 &= \sigma_{BA\ r}(s) - \sigma_{BA\ qe}(s) \equiv \int d^2\vec{b} \mu_{BA\ abs}(\vec{b}, s) \\
 &= \int d^2\vec{b} \int d^3\vec{w} |\Psi_{iB}(\vec{w})|^2 \int d^3\vec{u} |\Psi_{iA}(\vec{u})|^2 \\
 &\cdot \left\{ 1 - \prod_{k=1}^B \prod_{j=1}^A \left\{ 1 - \left[1 - |S_{hN}(\vec{b} - \vec{r}_{j\perp} + \vec{d}_{k\perp}, s)|^2 \right] \right\} \right\}
 \end{aligned}$$

where, as usual, $\sigma_{BA\ abs}(s)$ is the absorption (particle production) cross section as a function of the centre of mass energy, $\sigma_{BA\ T}(s)$ is the total one, $\sigma_{BA\ el}(s)$ the (coherent) elastic one and $\sigma_{BA\ qe}(s)$ the quasielastic (incoherent elastic) cross section. All of them can be computed out of the Glauber formalism.

The string interpretation for the Glauber cascade in nucleus-nucleus collision is similar to the one of hadron-nucleus reactions. In addition to valence-valence and sea-valence chains, sea-sea chains are also possible when both the projectile and target nucleon of a specific term in the Glauber expansion suffer more than one primary collisions.

Once the primary collision configuration is selected according to this formalism, the description proceeds pretty much in the same way as in the hadron-nucleus case. Chains are stretched and hadronized, the formation zone is taken into account and possible cascading in both the projectile and target nucleus is performed. At the end of the fast stages, spectator nucleons and nucleons which not escaped the system are grouped into projectile- and target-like residuals each one with the excitation energy resulting from the previous events. Evaporation/fission/fragmentation is then performed for both the projectile and target residuals. An example of an implementation along these ideas can be found in ⁽⁴³⁾.

CONCLUSIONS

Hadron interaction modelling is enough advanced to provide reliable estimates of particle production and propagation under most circumstances. Most of the basic features of nuclear interactions can be understood in terms of a general scheme where the fast, cascade, preequilibrium and equilibrium (“slow”) stages can be naturally concatenated, each one explaining for some of the experimental observables, and linked together in a coherent and self-consistent picture. This approach can be naturally exploited in MonteCarlo models which become very powerful tools in predicting interaction properties over a wide energy range and for a variety of applications, ranging from basic research to applied physics.

References

- [1] A. Fassò, A. Ferrari, J. Ranft, and P.R. Sala, *New developments in FLUKA modelling of hadronic and EM interactions*, in Proceedings of SARE-3, KEK-Tsukuba, H. Hirayama ed., May 7–9 1997, KEK report Proceedings 97-5, 32 (1997).
- [2] A. Fassò, A. Ferrari, J. Ranft, and P.R. Sala, *FLUKA: Status and Prospective for Hadronic Applications*, in Proceedings of the MonteCarlo 2000 Conference, Lisbon, October 23–26 2000, A. Kling, F. Barão, M. Nakagawa, L. Távora, P. Vaz eds., Springer-Verlag Berlin, 955 (2001).
- [3] A. Ferrari, and P.R. Sala, *The Physics of High Energy Reactions*, in Proceedings of Workshop on Nuclear Reaction Data and Nuclear Reactors Physics, Design and Safety, A. Gandini, G. Reffo eds., Trieste, Italy, April 1996, 2, 424 (1998).
- [4] A. Ferrari, P.R. Sala, *Physics processes in hadronic showers*, in Proceedings of the IX International Conference on Calorimetry in High Energy Physics, Annecy, October 9–14 2000, B. Aubert, J. Colas, P. Nédelec, L. Poggioli eds., Frascati Physics Series, 31 (2001).
- [5] S. Huber, and J. Aichelin, *Production of Δ - and N^* - resonances in the one-boson exchange model*, Nucl. Phys. **A573**, 587 (1994).
- [6] A. Engel, W. Cassing, U. Mosel, M. Schäfer, Gy. Wolf, *Pion-nucleus reactions in a microscopic transport model*, Nucl. Phys. **A572**, 657 (1994).
- [7] S. Teis, W. Cassing, M. Effenberger, A. Hombach, U. Mosel, Gy. Wolf, *Pion-Production in Heavy-Ion Collisions at SIS energies*, Z. Phys. A **357**, 451 (1997).
- [8] A. Capella, U. Sukhatme, C.-I. Tan and J. Tran Thanh Van, *Dual Parton Model*, Phys. Rep. **236**, 225 (1994).
- [9] A. Kaidalov, *The quark-gluon structure of the pomeron and the rise of inclusive spectra at high energies*, Phys. Lett. **B116**, 459 (1982).
- [10] A. Kaidalov, and K.A. Ter-Martirosyan, *Pomeron as quark-gluon strings and multiple hadron production at SPS-Collider energies*, Phys. Lett. **B117**, 247 (1982).
- [11] M. Adamus and 40 others, *Charged particle production in K^+p , π^+p and pp interactions at 250 GeV/c*, Z. Phys. **C39**, 311 (1988).
- [12] R.J. Glauber and G. Matthiae, *High-Energy Scattering of Protons by Nuclei*, Nucl. Phys. **B21**, 135 (1970).
- [13] R.J. Glauber, *High-energy collision theory*, in *Lectures in Theoretical Physics*, A.O. Barut, and W.E. Brittin eds, Interscience, NewYork (1959).
- [14] V.N. Gribov, *Glauber corrections and the interaction between high-energy hadrons and nuclei*, Sov. Phys. JETP **29**, 483 (1969).
- [15] V.N. Gribov, “Interaction of gamma quanta and electrons with nuclei at high energies”, Sov. Phys. JETP **30**, 709 (1970).
- [16] L. Bertocchi, *Graphs and Glauber*, Nuovo Cimento **11A**, 45 (1972).
- [17] C. De Marzo and 54 others, *Multiparticle production on hydrogen, argon, and xenon targets in a streamer chamber by 200-GeV/c proton and antiproton beams*, Phys. Rev. **D26**, 1019 (1982).

- [18] I.V. Ajinenko and 40 others, *Multiplicity distribution in K^+Al and K^+Au collisions at 250 GeV/c and a test of the multiple collision model*, Z. Phys. **C42**, 377 (1989).
- [19] E. Gadioli, and P.E. Hodgson, *Pre-equilibrium Nuclear Reactions*, Clarendon Press, Oxford, (1992).
- [20] V.F. Weisskopf, *Statistics and Nuclear Reactions*, Phys. Rev. **52**, 295 (1937).
- [21] A. Ferrari, P.R. Sala, J. Ranft, and S. Roesler, *Cascade particles, nuclear evaporation, and residual nuclei in high energy hadron-nucleus interactions*, Z. Phys. **C70**, 413 (1996).
- [22] N.Y.T. Porile, G.T. Cole and C. Rudy, *Nuclear reactions of silver with 25.2 GeV ^{12}C ions and 300 GeV protons*, Phys. Rev. **C19**, 2288 (1979).
- [23] L. Sihver, K. Aleklett, W. Loveland, P.L. McGaughey, D.H.E. Gross, and H.R. Jaqaman, *Gold target fragmentation by 800 GeV protons*, Nucl. Phys. **A543**, 703 (1992).
- [24] E. Gschwendtner, C.W. Fabjan, N. Hessey, T. Otto, and H. Vincke, *Measuring the photon background in the LHC experimental experiment*, Nucl. Instr. Meth. **A476**, 222 (2002).
- [25] H. Arnould and 65 others, *Experimental verification of neutron phenomenology in lead and transmutation by adiabatic resonance crossing in accelerator driven systems*, Phys. Lett. **B458**, 167 (1999).
- [26] G. Battistoni, A. Ferrari, T. Montaruli, and P.R. Sala, *Comparison of the FLUKA calculations with CAPRICE94 data on muons in atmosphere*, Astroparticle Physics, in press (2002).
- [27] J. Engel, T.K. Gaisser, P. Lipari, and T. Stanev, *Nucleus-nucleus collisions and interpretation of cosmic-ray cascades*, Phys. Rev. **D46**, 5013 (1992).
- [28] S.K. Charagi, and S.K. Gupta, *Coulomb-modified Glauber model description of heavy-ion reaction cross sections*, Phys. Rev. **C41**, 1610 (1990).
- [29] A. Bialas, M. Bleszynski, and W. Czyz, *Multiplicity distributions in nucleus-nucleus collisions at high energies*, Nucl. Phys **B111**, 461 (1976).
- [30] J. Aichelin, *'Quantum' molecular dynamics-a dynamical microscopic n-body approach to investigate fragment formation and the nuclear equation of state in heavy ion collisions*, Phys. Rep. **202**, 233 (1991) and references therein.
- [31] K. Niita, S. Chiba, T. Maruyama, T. Maruyama, H. Takada, T. Fukahori, Y. Nakahara, and A. Iwamoto, *Analysis of the (N,xN') reactions by quantum molecular dynamics plus statistical decay model*, Phys. Rev. **C52**, 2620 (1995).
- [32] G.F. Bertsch, and S. Das Gupta, *A guide to microscopic models for intermediate energy heavy ion collisions*, Phys. Rep. **160**, 189 (1988).
- [33] Gy. Wolf, G. Batko, W. Cassing, U. Mosel, K. Niita, and M. Schaefer, *Dilepton production in heavy-ion collisions*, Nucl. Phys. **A517**, 615 (1990).
- [34] Gy. Wolf, W. Cassing, and U. Mosel, *Eta and dilepton production in heavy-ion reaction*, Nucl. Phys. **A545**, 139c (1992).
- [35] B.A. Li, and W. Bauer, *Pion spectra in a hadronic transport model for relativistic heavy ion collisions*, Phys. Rev. **C44**, 450 (1991).
- [36] J. Ranft, *Dual parton model at cosmic ray energies*, Phys. Rev. **D51**, 64 (1995).
- [37] J. Ranft, *DPMJET version II.5, code manual*, hep-ph/9911232 (1999).
- [38] J. Ranft, *New features in DPMJET version II.5*, hep-ph/9911213 (1999).
- [39] J. Ranft, *Baryon stopping in high energy collisions and the extrapolation of hadron production models to Cosmic Ray energies*, hep-ph/0002137 (2000).
- [40] H. Sorge, H. Stöcker, and W. Greiner, *Relativistic Quantum Molecular Dynamics Approach to Nuclear Collisions at Ultrarelativistic Energies*, Nucl. Phys. **A498**, 567c (1989).
- [41] H. Sorge, H. Stöcker, and W. Greiner, *Poincaré Invariant Hamiltonian Dynamics: Modelling Multi-hadronic Interactions in a Phase Space Approach*, Ann. Phys. (N.Y.) **192**, 266 (1989).

- [42] H. Sorge, *Flavor production in Pb(160A GeV) on Pb collisions: Effect of color ropes and hadronic rescattering*, Phys. Rev. **C52**, 3291 (1995).
- [43] A. Ferrari, P.R. Sala, J. Ranft, and S. Roesler, *The production of residual nuclei in peripheral high energy nucleus-nucleus interactions*, Z. Phys. **C71**, 75 (1996).

FIGURE CAPTIONS

Fig. 1 : Leading two-chain diagram in DPM for $p - p$ scattering. The color (r→red, b→blue, g→green, \bar{r} →antired, \bar{b} →antiblue and \bar{g} →antigreen) and quark combination shown in the figure is just one of the allowed possibilities.

Fig. 2 : One of leading two-chain diagrams in DPM for $\pi^+ - p$ scattering. The color and quark combination shown in each figure is just one of the allowed possibilities.

Fig. 3 : Feynman x_F^* spectra of positive and negative particles from (π^+, p) at 250 GeV/c . Exp. data (symbols) from ⁽¹¹⁾.

Fig. 4 : Transverse momentum (p_t) spectra of positive and negative particles from (π^+, p) at 250 GeV/c . Exp. data (symbols) from ⁽¹¹⁾.

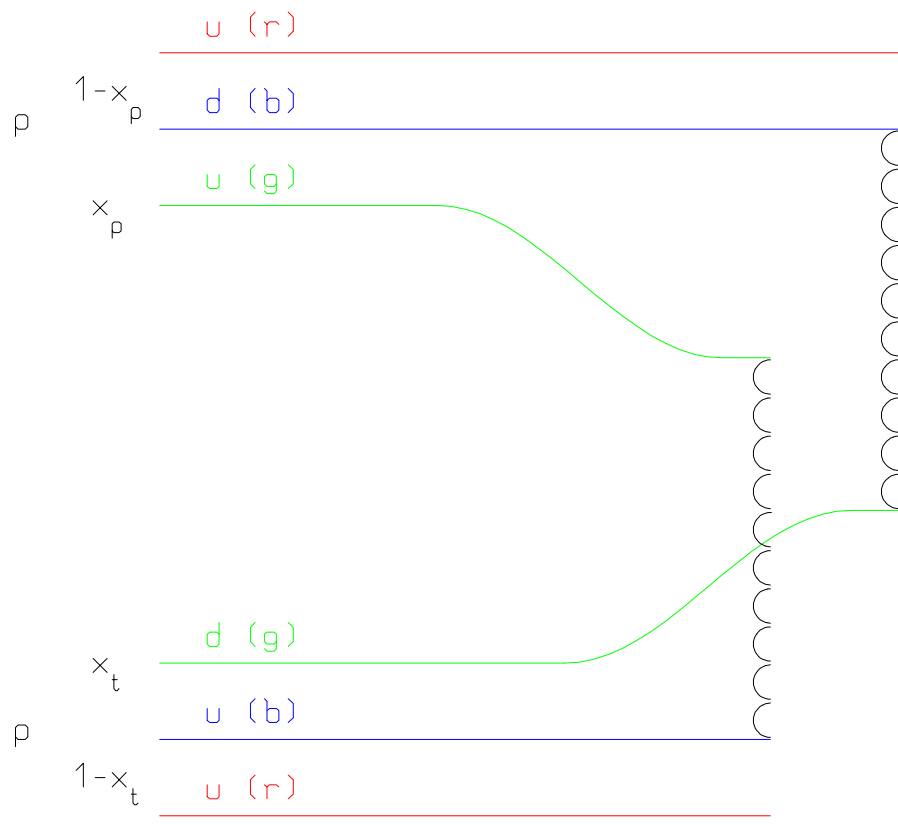
Fig. 5 : Leading two-chain diagrams in DPM for $p - A$ Glauber scattering with 4 collisions. The color and quark combinations shown in the figure are just one of the allowed possibilities.

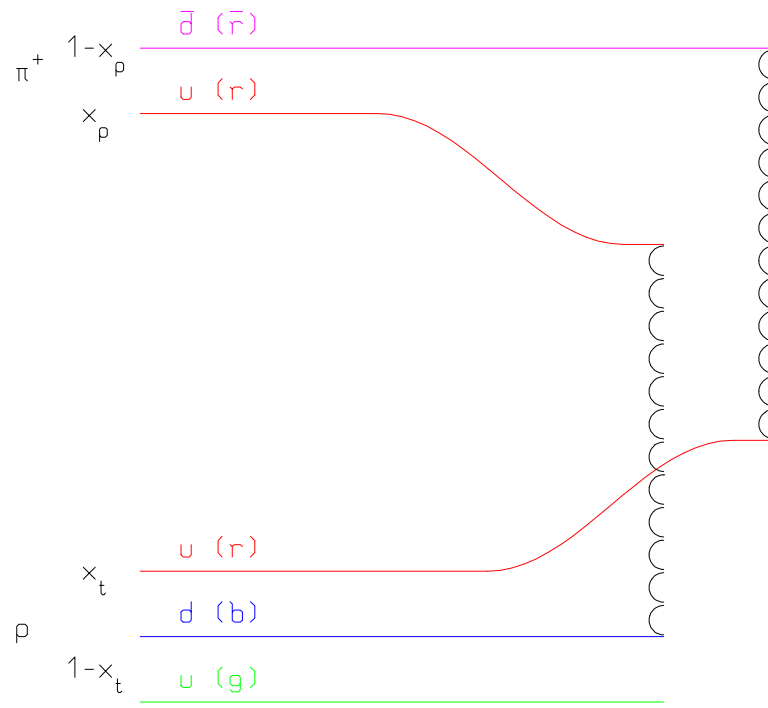
Fig. 6 : Rapidity distribution of charged particles produced in 200 GeV proton collisions on Hydrogen, Argon, and Xenon target, data from ⁽¹⁷⁾.

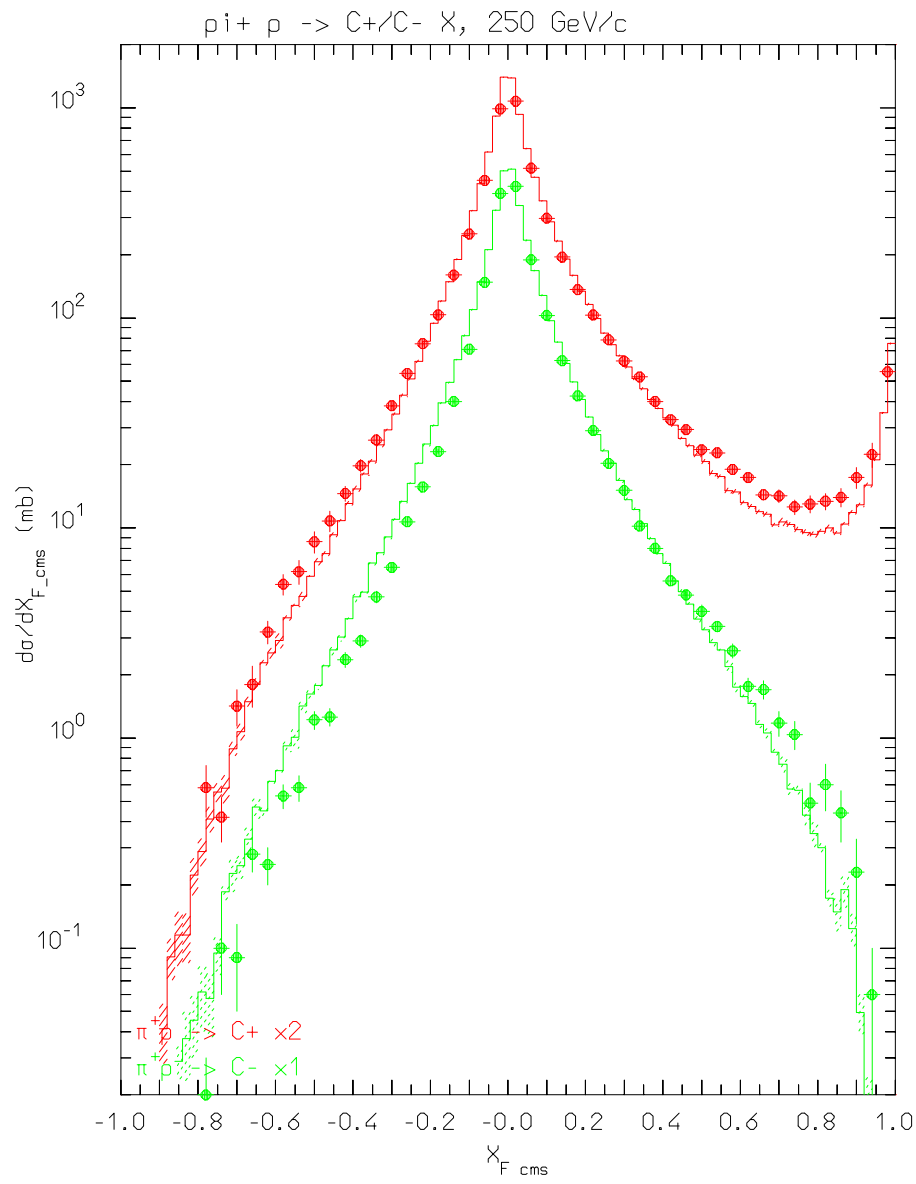
Fig. 7 : Multiplicity distribution of negative shower particles for 250 GeV/c K^+ on Aluminium and Gold targets (right), data from ⁽¹⁸⁾.

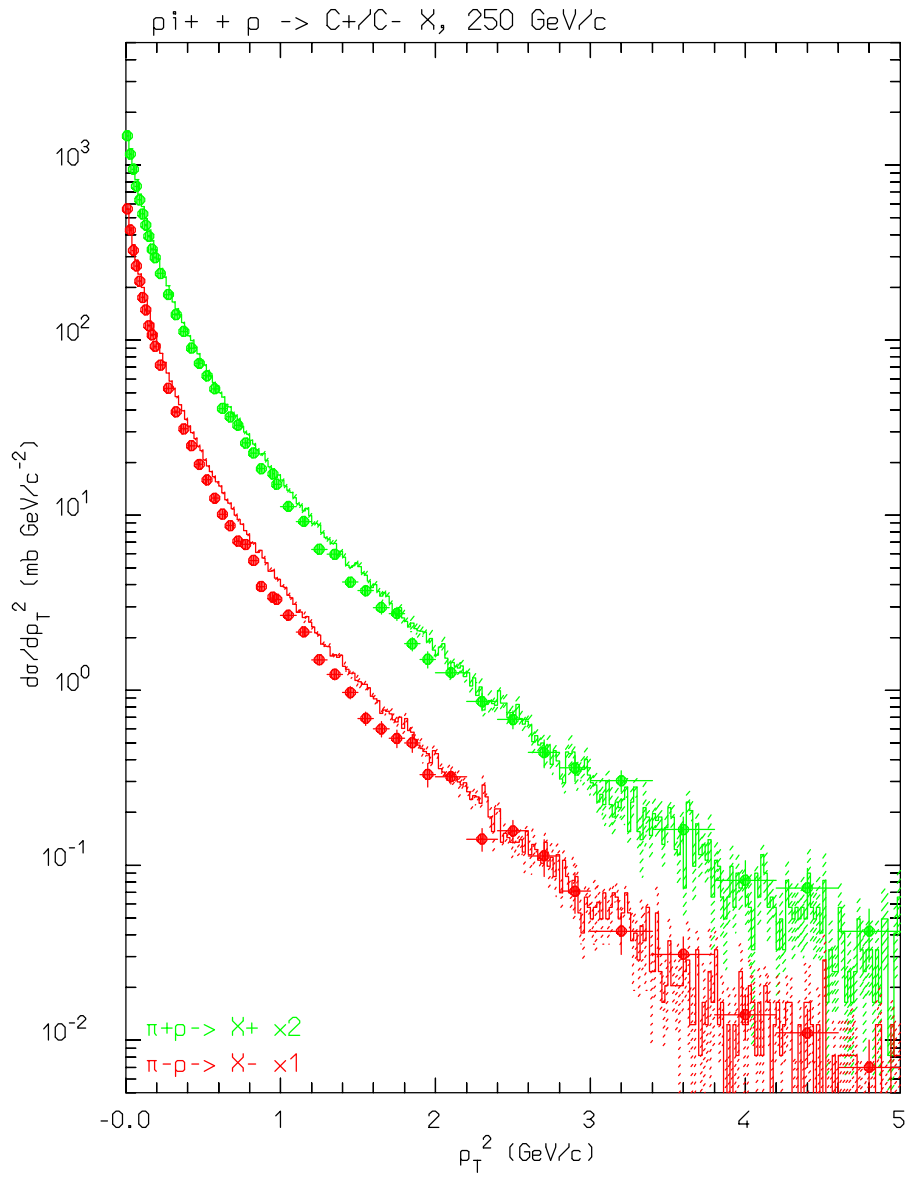
Fig. 8 : Shower, grey, and black tracks multiplicities for π^- (top) and protons (bottom) on emulsion, as a function of the projectile momentum. Open symbols are experimental data from various sources, full symbols are FLUKA results.

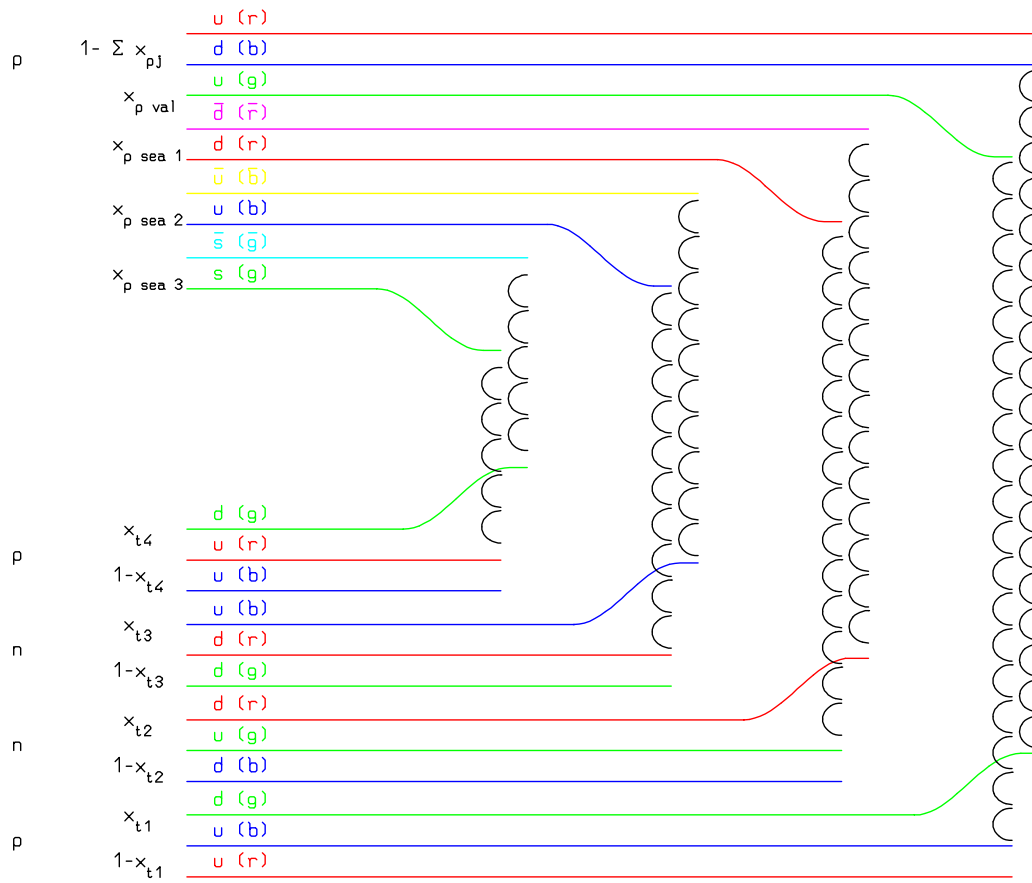
Fig. 9 : Residual nuclei mass distribution. Experimental data are from ⁽²²⁾ for silver, and ⁽²³⁾ for gold.

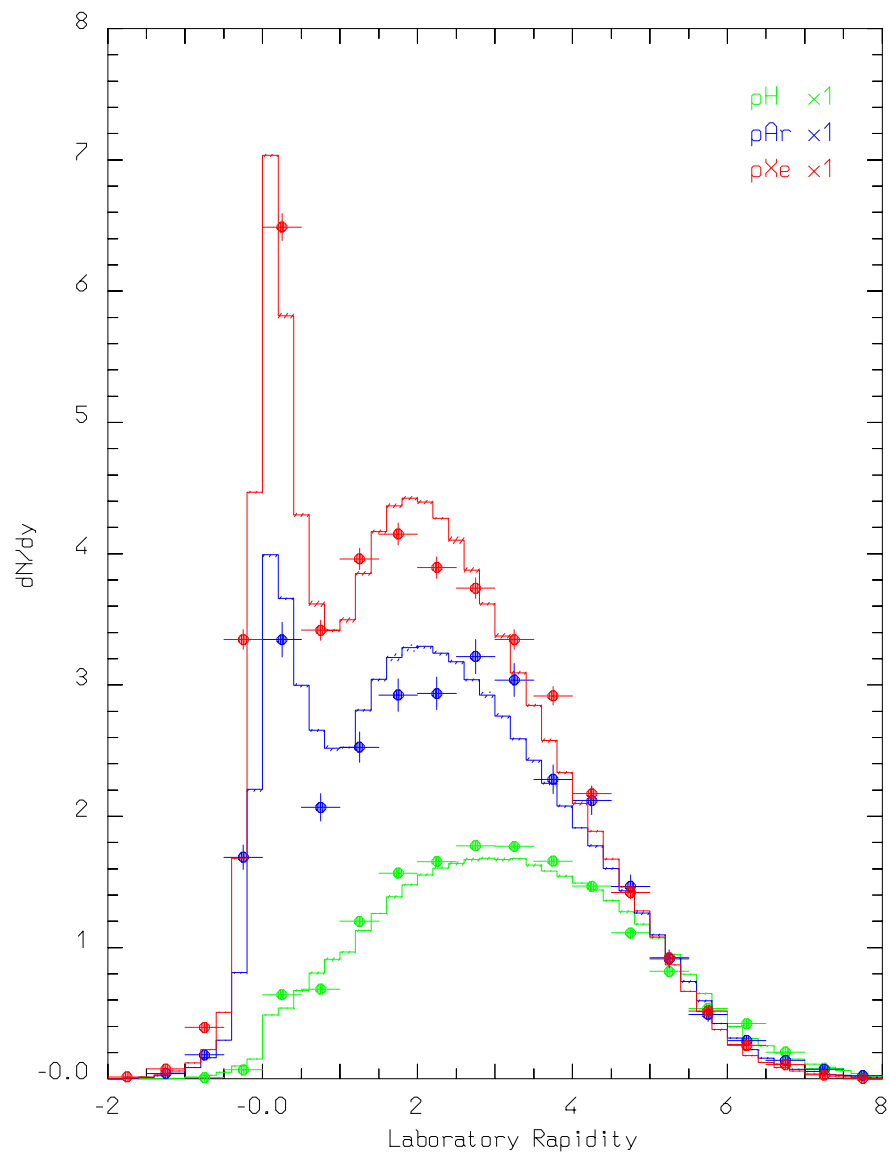


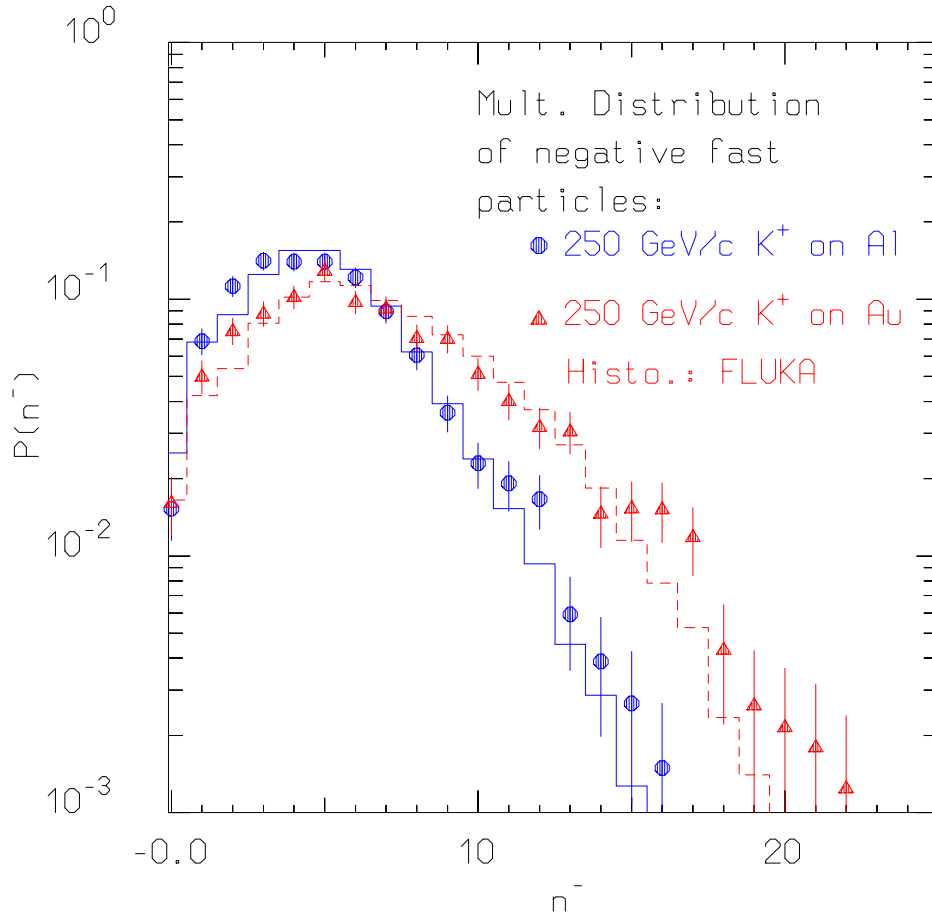


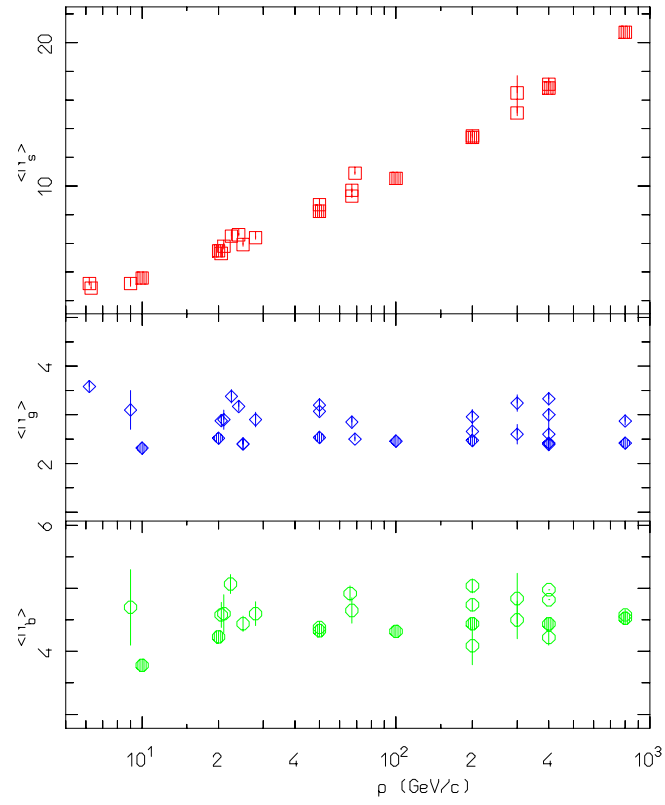
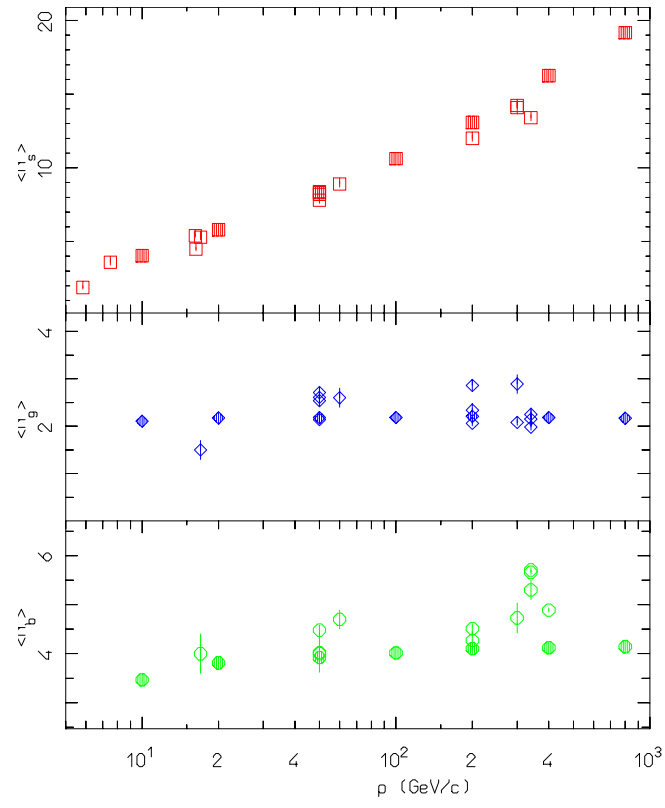












Residual nuclei distribution

